ISSN 1063-7788, Physics of Atomic Nuclei, 2022, Vol. 85, No. 1, pp. 96–107. © Pleiades Publishing, Ltd., 2022.
Russian Text © The Author(s), 2022, published in Yadernaya Fizika, 2022, Vol. 85, No. 1, pp. 76–87.

ELEMENTARY PARTICLES AND FIELDS
Experiment

Directional Observation of Particles of Cold Dark Matter (WIMP) in Experiments with Nuclear Track Emulsions and Other Tracking Detectors

A. M. Anokhina[1),2)*], I. D. Vidulin[1),2)], V. V. Gulyaeva[1)], E. V. Kurochkin[1),2)], T. M. Roganova[2)], E. D. Ursov[1),2)], and E. V. Khalikov[2)]

Received July 2, 2021; revised July 2, 2021; accepted July 2, 2021

Abstract—A scheme for modeling tracks of recoil nuclei from elastic scattering of hypothetical dark-matter weakly interacting massive particles (WIMP) is presented. Constraints on the possibility of directional detection of WIMP in experiments where light hydrogen nuclei and groups of C, N, and O nuclei, as well as fluorine nuclei, play the role of a target in the detector used are set. The number of WIMP interactions per unit mass of the detector was estimated by means of the micrOMEGAs software package for an inert doublet model. It is concluded that, for the purpose of visualizing tracks of recoil nuclei and, accordingly, accomplishing a directional detection of WIMP with lowest assumed masses of 4 to 10 GeV, preference should be given to target of lower density.

DOI: 10.1134/S1063778822010045

1. INTRODUCTION

Weakly Interacting Massive Particles (WIMP) are hypothetical particles that arise upon the extension of the Standard Model (SM) as candidates for dark matter particles. It is assumed that the Milky Way Galaxy is surrounded by a halo of WIMP with masses ranging between 0.4 and 10000 GeV.

Searches for WIMP have been performed vigorously over the past decade. The most stringent constraints on the cross section for WIMP–nucleon interaction in the case of WIMP masses higher than 10 GeV were set in the XENON1T experiment [1]: less than 10^{-46} cm^2 for WIMP of mass about 30 GeV and approximately 10^{-44} cm^2 for WIMP of mass 10^4 GeV. The mass range between 2 and 10 GeV was constrained by the results of the DarkSide experiment [2]: about 10^{-42} cm^2 for WIMP of mass about 4 to 5 GeV. It follows that, at the present time, it is reasonable to look for WIMP in the mass range extending up to 10 GeV, and such searches require employing detectors with a "light" working substance—that is, with an atomic number non differing markedly from ten.

The idea of directly detecting WIMP is based on the assumption that, in the course of its motion together with the Solar System, the Earth is blown around by a WIMP wind obeying a Maxwell velocity distribution and having an average velocity of about 220 km/s. In that case, WIMP should be involved in elastic interaction with a detector material, whereby recoil nuclei are produced, and it is proposed to detect them.

Some experiments are implemented in such a way that they make it possible to determine the directions of motion of recoil nuclei and, hence, to estimate the predominant direction of the WIMP flux prior to WIMP interaction with a target. The discovery of an anisotropy in the angular distribution of recoil nuclei (provided that the background signal is isotropic) may suggest that the Earth and Solar System move around the Milky Way Galaxy center within a dark-matter halo. Detectors proposed for visualizing tracks of recoil nuclei are highly sophisticated instruments, including time-projection multiwire proportional chambers [3], micro pattern gaseous detectors (MPGDs) [4], and graphene-based detectors for directional dark matter detection [5].

The maximum of the presumed velocity-direction distribution of WIMP approximately corresponds to the direction toward the Cygnus constellation. Background events associated with elastic interactions of neutrinos should either be isotropic (neutrinos from supernova explosions and atmospheric neutrinos) or correlate well with the position of the Sun (solar neutrinos). Therefore, the observation of an excess of the signal in the direction toward the Cygnus constel-

[1)]1 Место работы и/или адрес автора
[2)]2 Место работы и/или адрес автора
*E-mail: anokhannamsu@gmail.com

lation would be an unambiguous proof of the presence of dark matter in the form of a galactic halo [6].

In the present article, we describe a scheme for modeling tracks of recoil nuclei from the elastic WIMP scattering and set constraints on the possibility of directional detection of WIMP in an experiment where light nuclei of hydrogen (H) and groups of carbon, nitrogen, and oxygen nuclei (CNO groups), as well as fluorine nuclei (F), form a target in the detector used. The expected number of WIMP interactions per unit mass of the detector was estimated by means of the micrOMEGAs software package [7] for an inert doublet model (IDM) of WIMP. This model is compatible with the most recent experimental constraints in the WIMP mass range extending up to 10 GeV. As a result, it is concluded that, in order to visualize tracks of recoil nuclei and, hence, to accomplish directional detection of WIMP with lowest supposed masses between 4 and 10 GeV, preference should be given to a target of lower density.

2. SCHEME OF ELASTIC WIMP INTERACTION WITH DETECTOR MATERIAL AND ANGULAR AND ENERGY DISTRIBUTIONS OF RECOIL NUCLEI

We have considered three tracking-detector models that differ substantially in the sensitive-matter density. The first is the track-emulsion detector of density $\rho = 3.1$ g/cm^3 that was used in the NEWSdm experiment [8] and in which tracks were visualized by means of a NIT (nano imaging tracker) emulsion having a grain size of 40 to 80 nm [9]. In ordinary track emulsions, such as that used in the OPERA experiment devoted to searches for $\nu_\mu \to \nu_\tau$ neutrino oscillations [10], the emulsion-grain size was approximately 200 nm. For the second detector model, we considered 500 l of liquid propane C_3H_8 ($\rho = 0.495$ g/cm^3) in the bubble-chamber mode. The sensitive volume of the detector designed for the PICO experiment [11] was the third model. This is a bubble chamber containing 500 l of octafluoropropane C_3F_8 ($\rho = 1.601$ g/cm^3).

The elastic interaction of WIMP with target nuclei was described in a number of studies (see, for example [12, 13]). The respective scheme is shown in Fig. 1.

In order to model tracks of recoil nuclei in the detectors of directional experiments, one can use the double-differential distribution of recoil nuclei with respect to energy and direction in the form [13]

$$\frac{d^2R}{dEd\Omega} = \frac{\rho}{4\pi\mu^2 m}\hat{f}(w,\mathbf{w})\sigma_A(E), \qquad (1)$$

where $d\Omega = d\varphi d\cos\theta$, ρ is the local density of WIMP, m is the WIMP mass, M is the target-nucleus mass, $\mu = mM/(m+M)$ is is the reduced mass of the system formed by the target nucleus and WIMP, and

$$w = c\sqrt{\frac{ME}{2\mu^2}}$$

is the minimum WIMP velocity necessary for transferring the energy E to the target nucleus of mass M.

As in [13], we take the function $\hat{f}(w,\mathbf{w})$ in the form of a modified Maxwell distribution; that is,

$$\hat{f}(w,\mathbf{w}) = \int \delta(\mathbf{v}\cdot\hat{\mathbf{w}} - w)f(\mathbf{v})d^3v,$$

$$f(\mathbf{v}) = \frac{1}{(2\pi\sigma_V^2)^{3/2}}\exp\frac{-(\mathbf{v}-\mathbf{V})^2}{2\sigma_V^2},$$

where $\mathbf{v}$ is the WIMP velocity before interaction with the target nucleus, $\hat{\mathbf{w}} = \mathbf{w}/|\mathbf{w}|$ is the direction in which the recoil nucleus goes out after WIMP scattering off it, and $\mathbf{w}$ and $\mathbf{v}$ are specified with respect to the direction corresponding to the maximum of the distribution of WIMP velocities $\mathbf{V}$.

The cross section for WIMP scattering off a nucleus is the sum of the spin-independent (SI) and spin-dependent (SD) parts; that is,

$$\sigma_A(E) = \sigma_A^{\mathrm{SI}}(E) + \sigma_A^{\mathrm{SD}}(E).$$

Accordingly, the spin-dependent and spin-independent contributions can be separated in the distribution of recoil nuclei with respect to energy and direction. The spin-independent part of the cross section can be represented in the form

$$\sigma_A^{\mathrm{SI}} = \frac{4\mu^2}{\pi}(\lambda_p Z + \lambda_n(A-Z))^2 F_A^2(q),$$

where λ_p and λ_n are the amplitudes for WIMP scattering on a proton and a neutron, respectively; Z and A are, respectively, the charge and mass numbers of the scatterer nucleus; and F_A is the Helm form factor [14]

$$F_A^{\mathrm{Helm}}(q^2) = \frac{3j_1(qr_n)}{(qr_n)}\exp\frac{-(q^2s^2)}{2}.$$

Here, q is the momentum of the recoil nucleus, $r_n^2 = c^2 + \frac{7}{3}\pi^2a^2 - 5s^2$, $s = 1$ fm, $c = (1.23A^{1/3} - 0.6)$ fm, and

$$J_1(qr_n)\frac{\sin(qr_n)}{(q^2r_n^2)} - \frac{\cos(qr_n)}{(qr_n)}.$$

The spin-dependent (J_A is the spin of the nucleus) part of the cross section, $\sigma_n^{\mathrm{SD}}(E)$ [15],

$$\sigma_A^{\mathrm{SD}} = \frac{4\mu_A^2}{(2J_A+1)}(a_p^2S_{pp}(E) + a_n^2S_{nn}(E)$$

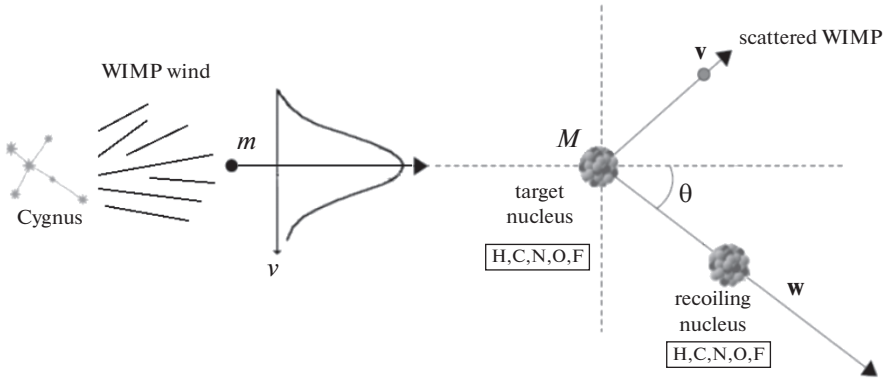

Fig. 1. Scheme of WIMP interaction with a target nucleus, whereby a recoil nucleus is produced. The WIMP velocities prior to the interaction are described by a Maxwell distribution with an average velocity of 220 km/s and $\sigma = 156$ km/s.

$$+ a_p a_n S_{pn}(E)),$$

is expressed in terms of the functions $S_{pp}(E)$, $S_{nn}(E)$, and $S_{pn}(E)$, which play the same role as the nuclear form factor $F(q^2)$ in the spin-independent case and have the form [16]

$$S_{pp}(E) = S_{00} + S_{11} + S_{01},$$
$$S_{nn}(E) = S_{00} + S_{11} - S_{01},$$
$$S_{pn}(E) = 2(S_{00} + S_{11}),$$

where S_{00}, S_{11}, and S_{01} are the nuclear spin structure functions [16]. If the spin of the nucleus is approximated by the odd-nucleon spin alone, then

$$S_{pp} = \frac{\lambda_n^2 J_A(J_A+1)(2J_A+1)}{\pi}, \quad S_{nn} = 0,$$
$$S_{pn} = 0;$$

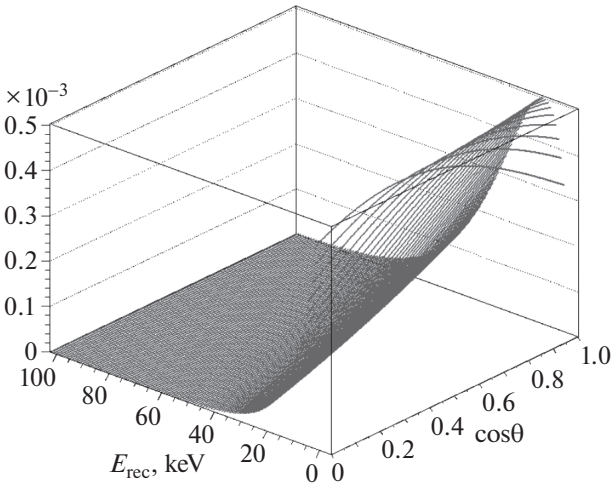

Fig. 2. Example of the two-dimensional probability-density used in modeling individual recoil nuclei with respective values of E_{rec} and $\cos\theta$. Carbon recoil nuclei produced in the interaction with WIMP having a mass of 60 GeV and an average velocity of 220 km/s ($\sigma =$ 156 km/s) are considered.

for nuclei featuring an odd proton and

$$S_{pp} = 0, \quad S_{nn} = \frac{\lambda_n^2 J_A(J_A+1)(2J_A+1)}{\pi},$$
$$S_{pn} = 0;$$

for nuclei featuring an odd neutron. The values of $\lambda_n^2 J_A(J_A+1)$ were taken from [17] and [12].

For target nuclei, we considered light H, C, N, and O nuclei entering into the composition of liquid propane (C_3H_8)—sensitive matter in the form of a nuclear emulsion in the detector for the NEWSdm experiment—as well as fluorine nuclei entering into the composition of octafluoropropane (C_3F_8)—sensitive matter in the detector for the PICO experiment. Hydrogen and fluorine nuclei have a spin of 1/2, while carbon and oxygen nuclei have zero spin.

Expression (1) was used to calculate the two-dimensional probability density for the distributions of various recoil nuclei with respect to the energy E_{rec} and with respect to the direction specified by $\cos\theta$. On the basis of these distributions, sets of individual recoil nuclei with specific values of E_{rec} and $\cos\theta$ were then simulated for WIMP that have various masses. An example of such a two-dimensional probability density is given in Fig. 2.

The absolute values of the cross sections for WIMP–nucleon interaction and the number of events per unit mass of matter in the detector were obtained by means of the micrOMEGAs software package [7] for specific models of WIMP.

Figures 3*a*, 3*b*, and 3*c* show examples of distributions of 10^5 modeled recoil nuclei of hydrogen, carbon, and fluorine with respect to E_{rec} (energy of recoil nuclei) and $\tan\theta_z$ (projection of the three-dimensional recoil-nucleus incidence angle onto the detector plane) for WIMP of mass 10 and 100 GeV. For the problem of determining the directions of tracks of recoil nuclei, it is precisely the projection of

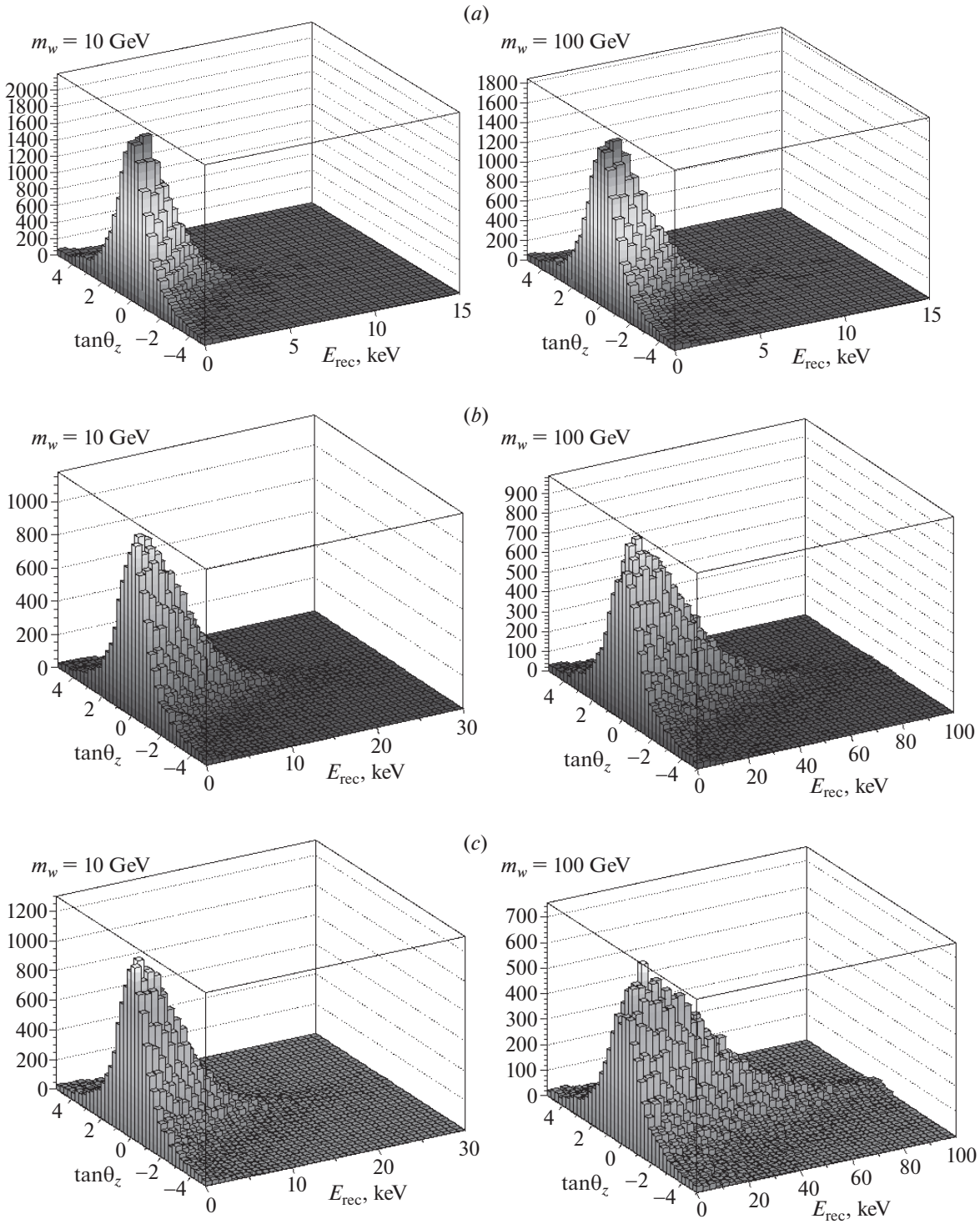

Fig. 3. Distributions of 10^5 (*a*) hydrogen, (*b*) carbon, and (*c*) fluorine recoil nuclei with respect to the energy, E_{rec}, and the projection of the three-dimensional recoil angle onto the detector-plane layer, $\tan\theta_z$, for WIMP of mass 10 and 100 GeV.

the angle onto the plane of the detector layer (for example, plane of emulsion plate) that represents most adequately the angle corresponding to the direction of the track that will be studied experimentally. It is noteworthy that the energies of hydrogen, carbon, and fluorine recoil nuclei are substantially different, but that the widths of the angular distributions of these nuclei for different WIMP masses are nearly indistinguishable. The widths of the distributions in question make it possible to estimate the sensitivity of the method to the directionality of the WIMP flux—the main task of the experiments devoted to a directional observation of dark-matter particles.

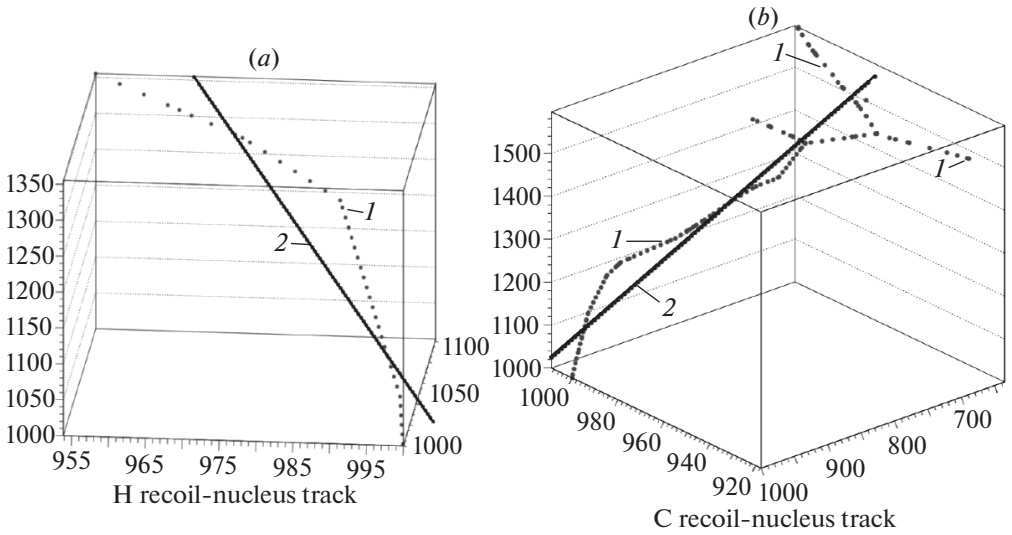

Fig. 4. Examples of tracks of hydrogen and carbon nuclei in a nuclear emulsion according to modeling on the basis of GEANT4, Nuclear Recoil Physics List, within the point-to-point scheme: (*1*) track points and (*2*) segment of the straight line plotted as a least squares fit to the tracks points. The values along the axes are given in nanometers.

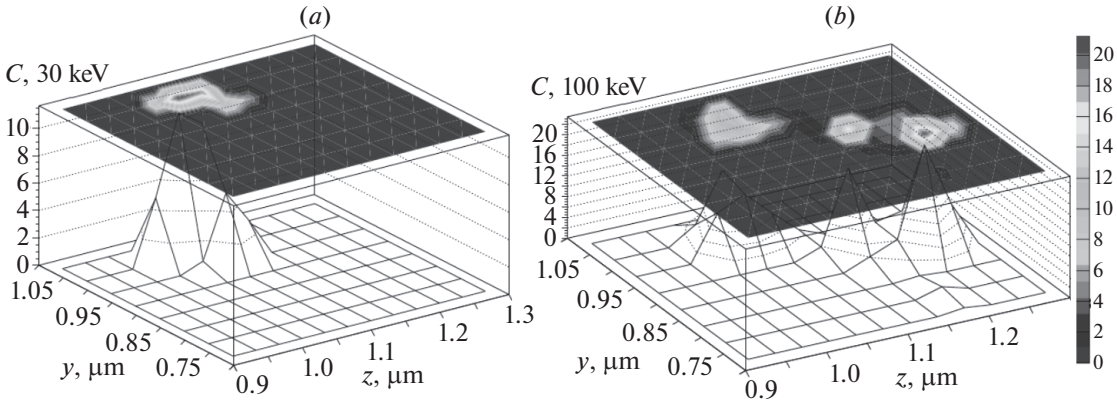

Fig. 5. Examples of tracks of carbon nuclei with energies of 30 and 100 keV in a nuclear emulsion according to modeling on the basis of GEANT4, Nuclear Recoil Physics List, within the scheme of energy-deposition calculation in three-dimensional voxels of matter.

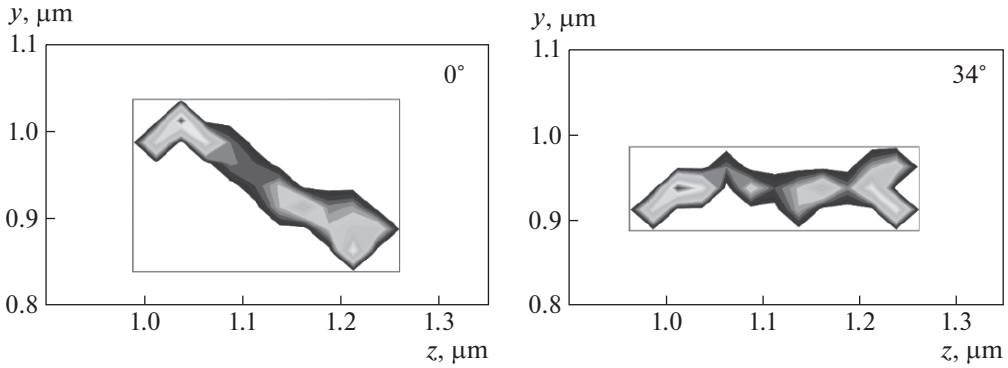

Fig. 6. (*a*) Original image of the track of a 100-keV carbon nucleus in a nuclear emulsion and (*b*) that rotated through an angle of 34°. For the rotated image, the longitudinal and the transverse size of the circumscribed rectangle are the track length and width, respectively. The scheme of modeling is that of calculating the energy deposition in elementary volumes of matter $25 \times 25 \times 25$ nm^3 in size.

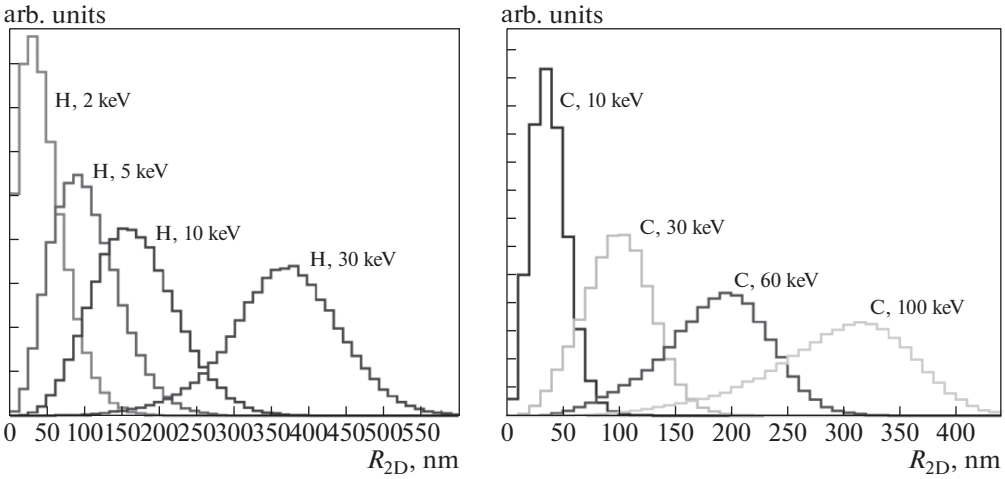

Fig. 7. Distributions of the lengths of tracks in a nuclear emulsion for fixed-energy (*a*) hydrogen and (*b*) carbon nuclei. The respective averages of the distributions are $\bar{R}_{2D}$ (2 keV) = 46.0, $\bar{R}_{2D}$ (5 keV) = 102.0, $\bar{R}_{2D}$ (10 keV) = 167.7, and $\bar{R}_{2D}$ (30 keV) = 364.7 (in nanometers) for hydrogen and $\bar{R}_{2D}$ (10 keV) = 38.9, R_{2D} (30 keV) = 99.2, $\bar{R}_{2D}$ (60 keV) = 185.1, and $\bar{R}_{2D}$ (100 keV) = 292.8 (in nanometers) for carbon.

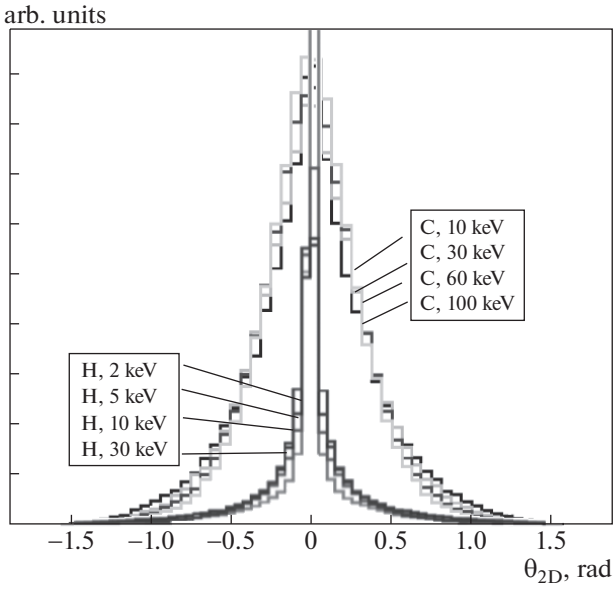

Fig. 8. Distributions of the angle between the initial direction of motion of a nucleus and the direction determined on the basis of track points in a nuclear emulsion for modeled tracks of hydrogen and carbon nuclei (10^5 events in each case). The respective variances of the distributions are D_θ (2 keV) = 0.3278, D_θ (5 keV) = 0.3455, D_θ (10 keV) = 0.3394, and D_θ (30 keV) = 0.2661 (in rad^2 units) for hydrogen and D_θ (10 keV) = 0.4018, D_θ (30 keV) = 0.3716, D_θ (60 keV) = 0.3456, and D_θ (100 keV) = 0.3233 (in rad^2 units) for carbon. These distributions demonstrate the degree of scattering undergone by recoil nuclei that traverse emulsion matter.

3. SCHEME FOR GEANT4-BASED SIMULATION OF TRACKS OF RECOIL NUCLEI IN DETECTOR MATERIALS

Upon the propagation of a recoil nucleus through the detector material, there arises an observable track, but it is necessary to consider that the recoil nucleus undergoes scattering and may deviate substantially from the initial direction. A simulation of tracks of fixed-energy nuclei and tracks of recoil nuclei from elastic WIMP scattering in the detector material was performed in two ways on the basis of the GEANT4 (Nuclear Recoil Physics List) code [18]. In the first case, tracks of nuclei were traced directly from point to point in a nuclear emulsion (or in another substance). Figure 4 illustrates the results obtained for the tracks of hydrogen and carbon nuclei by applying the first method of modeling. Individual dots represent points of a track; lines *2* are segments of the straight lines obtained as least squares fits to the track points. The track length and direction were determined from the lengths and orientation of these straight-line segments.

Upon the application of the point-to-point modeling method, the resulting track is a sequential chain of points in the track emulsion being considered, whereas the real track image obtained with the aid of a scanning optical microscope and a CCD camera appears to be a two-dimensional (for each scanned layer) matrix of pixels forming an image. In view of this, we proposed a different modeling scheme. It consists in measuring the energy deposition in unit emulsion volumes—voxels $25 \times 25 \times 25$ or $10 \times 10 \times 10$ nm^3 in size. This method is based on the assumption that the brightness (degree of darkening) of a

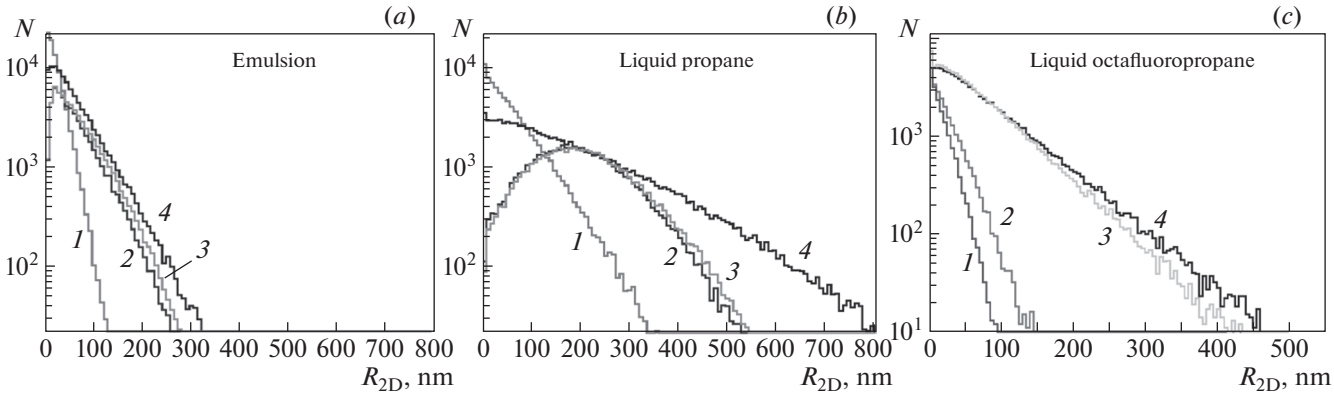

Fig. 9. Distributions of the lengths of tracks of hydrogen (H), carbon (C), and fluorine (F) recoil nuclei in (*a*) a nuclear emulsion, (*b*) liquid propane, and (*c*) liquid octafluoropropane for WIMP of mass $m_w = 10$ and 100 GeV. The GEANT4-dictated cut requiring that the minimum track length not fall short of 2 nm was imposed. In emulsion (*a*), $\bar{R}_{2D} = 19.41$ nm for C and $m_w = 10$ GeV (line *1*), $\bar{R}_{2D} = 58.24$ nm for H and $m_w = 10$ GeV (line *2*), $\bar{R}_{2D} = 63.12$ nm, for H and $m_w = 100$ GeV (line *3*), and $\bar{R}_{2D} = 55.39$ nm for C and $m_w = 100$ GeV (line *4*); in liquid propane (*b*), $\bar{R}_{2D} = 59.63$ nm for H and $m_w = 10$ GeV (line *1*), $\bar{R}_{2D} = 198.10$ nm for C and $m_w = 10$ GeV (line *2*), $\bar{R}_{2D} = 206.20$ nm for H and $m_w = 100$ GeV (line *3*), and $\bar{R}_{2D} = 179.20$ nm for C and $m_w = 100$ GeV (line *4*); and, in liquid octafluoropropane (*c*), $\bar{R}_{2D} = 13.76$ nm for F and $m_w = 10$ GeV (line *1*), $\bar{R}_{2D} = 23.48$ nm for C and $m_w = 10$ GeV (line *2*), $\bar{R}_{2D} = 66.85$ nm for F and $m_w = 100$ GeV (line *3*), and $\bar{R}_{2D} = 75.33$ nm for C and $m_w = 100$ GeV (line *4*).

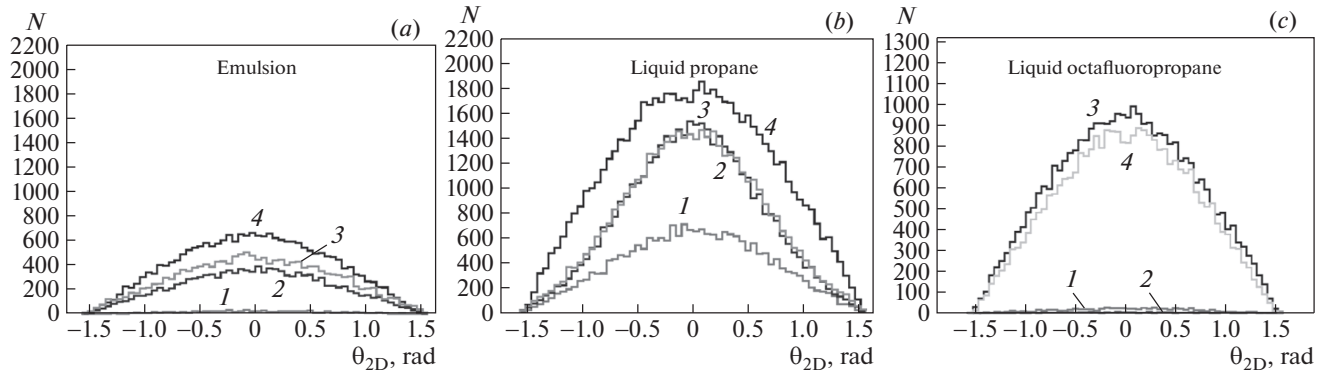

Fig. 10. Distributions of angles with respect to the direction toward the Cygnus constellation in (*a*) a nuclear emulsion, (*b*) liquid propane, and (*c*) liquid octafluoropropane for recoil nuclei of carbon (C) and fluorine (F) for WIMP of mass 10 and 100 GeV. The input number of events is 10^5 in each case. In emulsion (*a*), $N_{\rm cut} = 851$ for C and $m_w = 10$ GeV (line *1*); $N_{\rm cut} = 16312$ for H and $m_w = 10$ GeV (line *2*), $N_{\rm cut} = 12405$ for H and $m_w = 100$ GeV (line *3*), and $N_{\rm cut} = 22300$ for C and $m_w = 100$ GeV (line *4*); in liquid propane (*b*), $N_{\rm cut} = 22188$ for C and $m_w = 10$ GeV (line *1*), $N_{\rm cut} = 43179$ for H and $m_w = 10$ GeV (line *2*), $N_{\rm cut} = 65646$ for H and $m_w = 100$ GeV (line *3*), and $N_{\rm cut} = 43968$ for C and $m_w = 100$ GeV (line *4*); and, in liquid octafluoropropane (*c*), $N_{\rm cut} = 68$ for F and $m_w = 10$ GeV (line *1*), $N_{\rm cut} = 676$ for C and $m_w = 10$ GeV (line *2*), $N_{\rm cut} = 29779$ for F and $m_w = 100$ GeV (line *3*), and $N_{\rm cut} = 33595$ for C and $m_w = 100$ GeV (line *4*).

pixel in images obtained by means of a microscope is related to the energy deposited by the particle that forms the track in the emulsion (the higher the energy deposition, the higher the intensity of pixel's color). In order to obtain a flat image, the energy depositions in three-dimensional voxels were projected onto a plane. Figure 5 shows examples of images of tracks of carbon nuclei with energies of 30 keV (*a*) and 100 keV (*b*) in a nuclear emulsion.

The features of tracks that are modeled in the form of two-dimensional pixel images were calculated by two methods. The first method was applied to images of tracks of low-energy nuclei. These images form an exposed region that is not separated into fragments (see Fig. 5*a*). In that case, the distributions of energy depositions were approximated by a two-dimensional Gaussian function featuring five parameters (mathematical expectation, variances in two directions, and correlation coefficient). These parameters determined the characteristics of tracks (length, width, direction specified by the position of the major axis, and ellipticity).

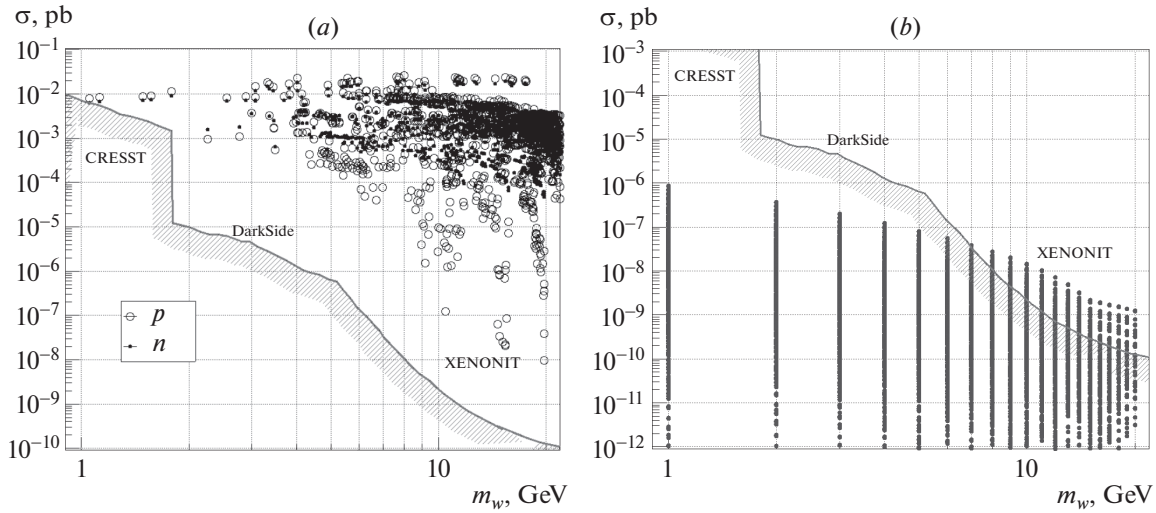

Fig. 11. Cross sections for the interactions of (*a*) NMSSM and (*b*) IDM dark-matter particles with nucleons along with the constraints set by the CRESST [29], DarkSide [28], and XENON1T [26] experiments.

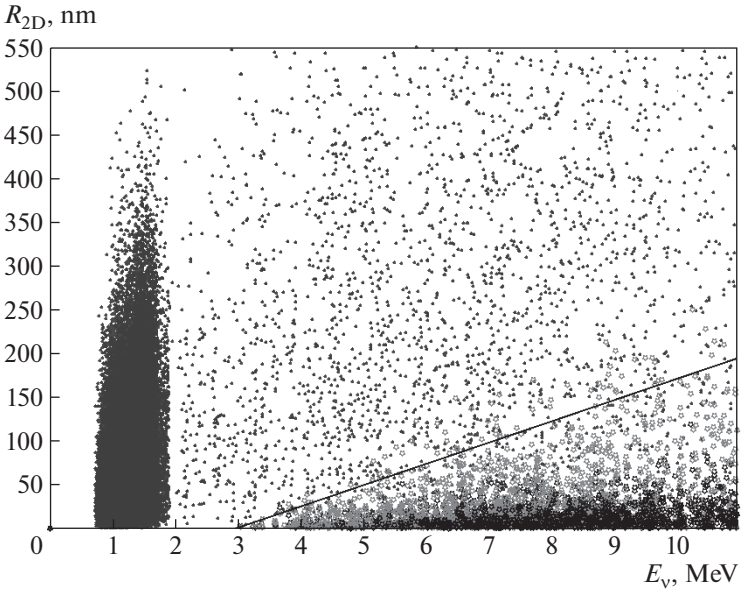

Fig. 12. Field of points corresponding to recoil nuclei of (dots) hydrogen and (asterisks) carbon and fluorine in a nuclear emulsion, liquid propane, and liquid octafluoropropane. The neutrino energy and lengths of track of recoil nuclei are plotted along the axes. The GEANT4-dictated cut of 2 nm on the minimum track length is imposed. The segment in the right bottom corner singles out the triangular region corresponding to the heavier nuclei of carbon and fluorine (asterisks).

The second method consists in the following. One first determines the coordinates of the center of gravity of the image and thereupon rotates step-by-step the image about the center of gravity through small angles. Each step involved determining the dimensions of an image along the coordinate axes as the lengths of the circumscribed-rectangle sides. Figure 6 shows an example of the original track image (0°) and the one rotated about the center of gravity through an angle of 34°. The track direction was determined as the angle of rotation of the spot about the x axis such that the size of the object along one of the axes (the respective projection of the object) was minimal (for example, along the y axis). The minimum projection itself determines the track width. The projection onto the other axis is the track length.

4. CHARACTERISTICS OF TRACKS OF RECOIL NUCLEI IN VARIOUS SUBSTANCES

At the first step, we studied the tracks of hydrogen H (2, 5, 10,and 30 keV) and carbon C (10, 30, 60,

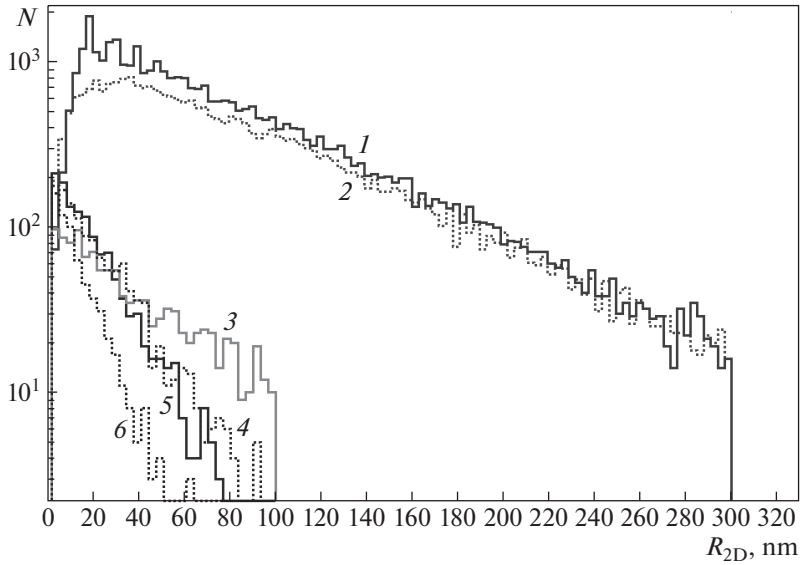

Fig. 13. Distributions of lengths of tracks of hydrogen (H), carbon (C), and fluorine (F) recoil nuclei in (*a*) a nuclear emulsion, (*b*) liquid propane, and (*b*) liquid octafluoropropane for solar neutrinos. The input number of events is 10^5 in each case. The cut of 2 nm is imposed on the minimum track length, and the number of events where the track is longer than 2 nm is denoted by $N_{\rm cut}$. The distributions in question lead to $\bar{R}_{2D} = 73.09$ nm and $N_{\rm cut} = 36443$ for H and liquid propane (line *1*), $\bar{R}_{2D} = 79.06$ nm and $N_{\rm cut} = 26826$ for H and emulsion (line *2*), $\bar{R}_{2D} = 46.94$ nm and $N_{\rm cut} = 1372$ for C and liquid propane (line *3*), $\bar{R}_{2D} = 21.77$ nm and $N_{\rm cut} = 1344$ for C and octafluoropropane (line *4*), $\bar{R}_{2D} = 18.06$ nm and $N_{\rm cut} = 1351$ for C and emulsion (line *5*), and $R_{2D} = 11.75$ nm and $N_{\rm cut} = 721$ for F and octafluoropropane (line *6*).

and 100 keV) nuclei having fixed energies and initially propagating in nuclear-emulsion matter of density $\rho = 3.1$ g/cm^3 as a parallel flux. It was necessary to perform this simulation in order to estimate the degree of scattering of recoil nuclei and the resulting lengths of tracks of nuclei that have different energies. The distributions with respect to lengths of track projections onto the plane of the detector layer (emulsion plate in the cases being considered), R_{2D}, for hydrogen and carbon nuclei of various energy are shown in Fig. 7.

The distributions of the angle determined on the basis of track points with respect to the initial direction of motion of the nucleus are shown in Fig. 8, the scattering of nuclei being characterized by the variance D_θ of these distributions.

The main objective of the present study is to explore the features of tracks of recoil nuclei from WIMP of various mass in substances of various density with allowance for the physics problem of determining the track direction.

The distributions of tracks of recoil nuclei of hydrogen, carbon, and fluorine in the lengths and angles with respect to the direction toward the Cygnus constellation are shown in Figs. 9 and 10 according to modeling based on the GEANT4 StandardNR Physics List. In that specific case, the nuclear emulsion exemplifies dense matter: $\rho = 3.1$ g/cm^3. As an alternative detector material, we have considered liquid propane, which has a density of $\rho = 0.493$ g/cm^3, which is substantially lower than that of a nuclear emulsion and which can find applications as a tracking detector in the bubble-chamber mode; we have also considered the target of the PICO experiment detector [11]—this is liquid octafluoropropane C_3F_8 of density $\rho = 1.601$ g/cm^3.

The initial energies and directions of recoiling nuclei (H, C, and F) were determined on the basis of the two-dimensional probability densities in (1) for WIMP of mass 10 and 100 GeV. The distributions of 10^5 H, C, and F nuclei with respect to the initial energy $E_{\rm rec}$ and with respect to the direction specified by $\tan\theta_z$ are shown in Fig. 3.

The distributions of the tracks of recoil nuclei of hydrogen, carbon, and fluorine with respect to the lengths, R_{2D}, in the materials being considered are presented in Fig. 9.

As was indicated above, an emulsion characterized by an ultrasmall grain size down to 40 nm was used in the NEWSdm experiment. In order that the directions of the tracks could be determined in scanning the emulsion, the tracks should have an elliptic shape. This means that the longitudinal size of a track should be larger than 40 nm. In order to estimate the number of events, one can constrain the minimal length of modeled tracks (for example, by two grain

sizes) and calculate the number of tracks whose direction can be determined. The distributions in Fig. 9 were obtained upon requiring that the minimum track length be 2 nm; this specific constraint was dictated by the scenario of the GEANT4-based simulation.

A substantially lower density of propane makes it possible to visualize a sizably greater number of tracks of recoil nuclei in relation to tracks in emulsions which are denser. Since initial WIMP are distributed in angles rather widely (Figs. 3*a*–3*c*), the angular distributions of tracks of recoil nuclei accordingly turn out to be wide (see Fig. 10). In the case being considered, the distributions were constructed upon cutting off track lengths smaller than two grain sizes—80 nm. The caption under Fig. 10 indicates the number of tracks that remained in three substances differing in density after imposing this cut on the track lengths, N_{cut}.

Figures 9 and 10 illustrate the fact that WIMP of low mass (10 GeV) are unable to interact efficiently with C and F nuclei, generating tracks of recoil nuclei with a length not smaller than about 100 nm in octafluoropropane; at the same time, WIMP of mass 100 GeV can do this. It follows that the PICO detector, as well as the detector of the XENON1T experiment, demonstrates a higher sensitivity to WIMP of mass within or about 100 GeV. The angular distribution of tracks of recoil nuclei are similar in shape in less dense (C_3H_8) and denser (emulsion) matter, but cuts on the track length for WIMP of mass 10 GeV impoverish much more strongly the statistics of recoil fluorine nuclei, which are heavier.

The lengths and angular distributions of tracks of recoil nuclei from WIMP of various mass in NIT emulsions are presented in [19] according to calculations on the basis of the SRIM (Stopping and Range of Ions in Matter) software package. Also, an additional modeling scenario that takes into account the crystal structure of grains in emulsions was considered there. In relation to the GEANT4 StandardNR model used here, modeling with the aid of the SRIM code leads, as was indicated in [19], to somewhat longer tracks of recoil nuclei and to wider angular distributions of the tracks. According to [20], the average value of the track-length distribution in a standard nuclear emulsion is $(3.25 \pm 1.73) \times 10^2$ μm for WIMP of mass 10 GeV and $(9.46 \pm 4.57) \times 10^2$ μm for WIMP of mass 100 GeV.

5. MODEL OF COLD DARK MATTER (WIMP)

The micrOMEGAs 5.2.4 software package [21] was used to estimate quantitatively the signal from WIMP. This is a code for calculating the properties of cold dark matter for various supersymmetric extensions of the Standard Model (SM). At the present time, it is commonly believed that the Minimal Supersymmetric Standard Model (MSSM) [22], in which a spin-1/2 particle in the form of a linear combination of bino, wino, higgsino1, and higgsino2 (superpartners) is a candidate for the dark-matter particle, is excluded definitively as a model of cold dark matter.

In order to estimate cross sections for WIMP interactions with matter, use is made of the Next-to-Minimal Supersymmetric Standard Model (NMSSM) [23, 24] and the Inert Doublet Model (IDM) [25] for minimal WIMP masses of about (or below) 10 GeV, since higher masses were ruled out by experiments, including XENON1T [26]. Within NMSSM, a spin-1/2 particle that, in just the same way as in MSSM, is a linear combination of bino, wino, higgsino1, and higgsino2 but with an additional contribution from the new superpartner singlino is a candidate for the dark-matter particle.

The supergravity (SUGRA) scenario was considered within NMSSM [27].

The WIMP mass, the quantity Ωh^2, and the cross sections σ_p and σ_n for the interaction of dark-matter particles with nucleons (protons and neutrons, respectively) were calculated for wide ranges of primary model parameters.

The calculations for a wide set of primary parameters revealed (see Fig. 11*a*) that NMSSM is also nearly excluded for WIMP masses of several GeV units and above this by XENON1T data [26]. The DarkSide [28] and CRESST [29] experiments set limits on the cross sections for WIMP–nucleon interaction for WIMP masses of about 1 GeV.

It turned out that IDM [25] is the most promising model from the point of view of experimental constraints. This model involves four new physical states: two charged, H^{+-}, and two neutral, H^0 and A^0, ones; of them, each may be a cold-dark-matter particle. For such a candidate, we have considered H^0 as the lightest inert particle. Figure 11*b* shows that there are many IDM versions compatible with experimental constraints for WIMP masses not higher than 10 GeV.

For our numerical estimations, we chose WIMP of mass 10 GeV. We also chose the IDM version where the cross section for WIMP–nucleon interaction has the maximum possible value that is compatible with modern experimental and cosmological constraints. The respective values of the number of events per day in 1 kg of the target are presented in summarizing Table 1.

Table 1. Estimated numbers of events associated with elastic scattering of WIMP (N_{wimp}) and solar neutrinos (N_ν) in nuclear emulsion, liquid propane (C_3H_8) and liquid octafluoropropane (C_3F_8)

Detector material (mass, volume)	N_{wimp} (per year in 1 kg of material)	N_{wimp} (per year in total volume of detector)	N_ν (per year in total volume of detector)
Emulsion, 30 kg	3.14×10^{-2}	0.94	$<2.51 \times 10^{-2}$
C_3H_8, 500 л	4.82×10^{-2}	23.75	$<2.32 \times 10^{-2}$
C_3F_8, 500 л	2.42×10^{-1}	194.0	$<4.47 \times 10^{-2}$

6. ELASTIC INTERACTION OF SOLAR NEUTRINOS WITH DETECTOR MATERIAL AS A DIRECTIONAL BACKGROUND TO OBSERVATION OF WIMP

In the present study, we consider the possibility of analyzing directions and lengths of tracks of recoil nuclei from WIMP for the problem of searches for an excessive signal in the direction toward the Cygnus constellation. Recoil nuclei from the elastic interaction of solar neutrinos with nuclei of the detector material may be a directional background in this problem. The expressions for the cross section for elastic neutrino–nucleus scattering that were used to estimate the neutrino background can be found, for example, in [30]. We modeled the energies of solar neutrinos according to the respective spectrum from [31], starting from the energy of 0.5 MeV.

The points corresponding to recoil nuclei in less dense (C_3H_8 and C_3F_8) and denser (emulsion) substances in the plane spanned by the variables of the neutrino energy and the length of the recoil-nucleus track are shown in Fig. 12.

This field of points illustrates the fact that tracks of length larger than 2 nm can be formed by hydrogen recoil nuclei from the elastic interaction of neutrinos with energies in the region of $E_\nu > 0.8$ MeV and by carbon and fluorine recoil nuclei from the interaction of neutrinos with energies in the region of $E_\nu > 3$ MeV. The contribution of carbon recoil nuclei to the background is minimal. A characteristic accumulation of points in the region of solar-neutrino energies around 1 to 2 MeV is associated with the shape of the input neutrino spectrum.

Figure 13 shows the track-length distributions of recoil nuclei from solar neutrinos in C_3H_8 and C_3F_8 and in a nuclear emulsion. The requirement that a nanoemulsion be sensitive to directions of recoil-nucleus tracks constrains the track lengths to be larger than 60 to 80 nm, whereupon it becomes clear that hydrogen nuclei make a dominant contribution to the directional signal from solar neutrinos.

7. RESULTS AND CONCLUSIONS

We have estimated the directional annual signal from WIMP of mass 10 GeV in 30 kg of a nuclear emulsion, 500 l of liquid propane, and 500 l of liquid octafluoropropane. With an eye to the problem at hand, which consists in determining the directions of tracks of recoil nuclei, we required that, in all of the substances under consideration, the minimum track length be larger than 80 nm. It has been found that approximately one directional event per year induced by the interaction of WIMP treated as a dark-matter particle of the inert doublet model (IDM), which is not ruled out by modern experimental constraints, is expected in the sensitive emulsion volume being studied. In order to detect about ten directional events associated with WIMP, it is therefore necessary to expose and process as much as 300 kg of emulsion but this would require considerable material and human resources.

In C_3H_8 and C_3F_8 targets consisting of light nuclei exclusively, which provide longer tracks of recoil nuclei, we expect, respectively, 24 and 194 WIMP events per year.

The estimates presented above give grounds to conclude that, in view of the available experimental constraints on the cross sections for elastic WIMP–nucleus interaction, the use of lighter and less dense targets as a sensitive detector element is preferable in addressing the problem of directional direct detection. These results are listed in Table 1 along with the estimated numbers of events from solar neutrinos.

FUNDING

This work was supported by Interdisciplinary Scientific and Educational School of Moscow State University Fundamental and Applied Studies of Cosmos. The work of E.D. Ursov was supported by a grant (no. 20–2–9–26–1) from Basis Foundation.

REFERENCES

1. XENON Collab. (E. Aprile et al.), Phys. Rev. Lett. **119**, 181301 (2017).
2. DarkSide Collab. (P. Agnes et al.), Phys. Rev. Lett. **121**, 081307 (2018).
3. K. N. Abazajian, M. A. Acero, S. K. Agarwalla, A. A. Aguilar-Arevalo, C. H. Albright, S. Antusch, C. A. Arguelles, A. B. Balantekin, G. Barenboim, V. Barger, P. Bernardini, F. Bezrukov, O. E. Bjaelde, S. A. Bogacz, N. S. Bowden, et al., arXiv: 1204.5379 [hep-ph].
4. Y. Giomataris, Ph. Rebourgeard, J. P. Robert, and G. Charpak, Nucl. Instrum. Methods Phys. Res., Sect. A **316**, 29 (1996).
5. Shang-Yung Wang, Eur. Phys. J. C **79**, 561 (2019). https://doi.org/10.1140/epjc/s10052-019-7071-2

6. A. M. Green, in *Proceedings of the 220th IAU Symposium* (Cambridge Univ. Press, Cambridge, 2004).
7. G. Belanger, F. Boudjema, and A. Pukhov, arXiv: 1402.0787.
8. NEWSdm. Collab. (N. Agafonova et al.), Eur. Phys. J. C **78**, 758 (2018). doi 10.1140/epjc/s10052-018-6060-1
9. T. Asada, T. Naka, T. Kuwabara, and M. Yoshimoto, Prog. Theor. Exp. Phys. **2017**, 063H01 (2017). doi 10.1093/ptep/ptx076
10. OPERA Collab. (N. Agafonova et al.), Phys. Rev. Lett. **120**, 211801 (2018).
11. PICO Collab. (C. Amole et al.), Phys. Rev. D **100**, 022001 (2019).
12. J. D. Lewin and P. F. Smith, Astropart. Phys. **6**, 87 (1996).
13. M. S. Alenazi and P. Gondolo, Phys. Rev. D **77**, 043532 (2008).
14. P. F. Smith and J. D. Lewin, Phys. Rep. **187**, 203 (1990). doi 10.1016/0370-573(90)90081-C
15. C. Savage, P. Gondolo, and K. Freese, Phys. Rev. D **70**, 123513 (2004).
16. J. Engel, Phys. Lett. B **264**, 114 (1991).
17. J. Ellis and R. A. Flores, Phys. Lett. B **263**, 259 (1991).
18. http://geant4.web.cern.ch/geant4/UserDocumentation/UsersGuides/PhysicsReference Manual/for/PhysicsReferenceManual.pdf.
19. A. Alexandrov, G. de Lellis, A. di Crescenzo, A. Golovatiuk, and V. Tioukov, J. Cosmol. Astropart. Phys. **2021** (04), 47 (2021).
20. C. Couturier, J. P. Zopounidis, N. Sauzet, F. Naraghi, and D. Santos, J. Cosmol. Astropart. Phys. **2017** (01), 027 (2017). https://doi.org/10.1088/1475-7516/2017/01/027
21. D. Barducci, G. Bélanger, J. Bernon, F. Boudjema, J. Da Silva, A. Goudelis, S. Kraml, U. Laa, A. Pukhov, A. Semenov, and B. Zaldivar, the Manual. https://lapth.cnrs.fr/micromegas/.
22. A. Bottino, N. Fornengo, and S. Scopel, Phys. Rev. D **67**, 063519 (2003).
23. Tao Han, Zhen Liu, and Shufang Su, J. High Energy Phys. **1408**, 093 (2014). https://doi.org/10.1007/JHEP08(2014)093
24. U. Ellwanger and C. Hugonie, Comput. Phys. Commun. **177**, 399 (2007).
25. M. Gustafsson, arXiv: 1106.1719. https://doi.org/10.22323/1.114.0030
26. XENON Collab. (E. Aprile et al.), Phys. Rev. Lett. **119**, 181301 (2017).
27. G. K. Chakravarty, G. Gupta, G. Lambiase, and S. Mohanty, Phys. Lett. B **760**, 263 (2016); arXiv: 1604.02556
28. DarkSide Collab. (P. Agnes et al.), Phys. Rev. Lett. **121**, 081307 (2018).
29. CRESST Collab. (A. H. Abdelhameed et al.), Phys. Rev. D **100**, 102002 (2019).
30. C. A. J. O'Hare, A. M. Green, J. Billard, E. Figueroa-Feliciano, and L. E. Strigari, Phys. Rev. D **92**, 063518 (2015).
31. W. C. Haxton, R. G. Hamish Robertson, and A. M. Serenelli, Ann. Rev. Astron. Astrophys. **51**, 21 (2013).